Chemical Geology 403 (2015) 42–51

Contents lists available at ScienceDirect

Chemical Geology

journal homepage: www.elsevier.com/locate/chemgeo

High-resolution line-scan analysis of resin-embedded sediments using laser ablation-inductively coupled plasma-mass spectrometry (LA-ICP-MS)

Rick Hennekam [a,*,1], Tom Jilbert [b], Paul R.D. Mason [a], Gert J. de Lange [a], Gert-Jan Reichart [a,c]

[a] Department of Earth Sciences — Geochemistry, Utrecht University, 3584 CD Utrecht, The Netherlands
[b] Department of Environmental Sciences, Helsinki University, P.O. Box 65, 00014 Helsinki, Finland
[c] Geology Department, Royal Netherlands Institute for Sea Research (NIOZ), 1797 SZ Den Hoorn, Texel, The Netherlands

ARTICLE INFO

Article history:
Received 22 August 2014
Received in revised form 20 February 2015
Accepted 8 March 2015
Available online 14 March 2015

Editor: Michael E. Böttcher

Keywords:
LA-ICP-MS
Resin-embedded sediment
Laminated sediments
High-resolution paleoclimate

ABSTRACT

Laser ablation-inductively coupled plasma-mass spectrometry (LA-ICP-MS) line-scanning is a promising technique for producing high-resolution (μm-scale) geochemical records on resin-embedded sediments. However, this approach has not yet been thoroughly tested on sediment samples of known elemental compositions. Here, we address this through the analysis of resin-embedded quartz, calcite, and clay (montmorillonite) sediments spiked with Al, V, Mo, and Ba across a range of concentrations. LA-ICP-MS spot analyses on these samples were compared to data independently obtained by conventional techniques: solution nebulization-ICP-optical emission spectroscopy (SN-ICP-OES), SN-ICP-MS, and X-Ray Fluorescence on fused glass beads. Data were reported as (log-)ratios of the analyte elements normalized to Ca, Si, and Al for calcite, quartz and clay respectively to correct for varying ablation yields. Our LA-ICP-MS data demonstrate close agreement to within 6% of the reference values determined by the conventional techniques, with high correlation coefficients ($R^2 \approx 1.0$) across the full range of concentrations, and high precision (<3% relative standard deviations after three repeated analyses). Barium was hosted in both aluminosilicates and carbonates in the clay matrix, giving different yields (elemental fractionation), and leading to variable accuracy (mean deviation of 15%). A selection of the spiked sediments was used to produce artificial laminated sediments to further test the effects of line scanning on LA-ICP-MS accuracy and precision in resin-embedded samples. It appears that LA-ICP-MS line-scan analyses have good accuracy (deviations from the reference values generally <5%) and high precision (relative standard deviations of repeated analyses on the same sample generally <5%) for our target elements. Moreover, the LA-ICP-MS line-scanning closely records the alternating geochemical profiles of our artificial laminations. However, calcium showed a clear tailing signal at the transition from a calcite to a quartz layer, indicating that geochemical signals can be smeared at transitions to sediment layers devoid of analyte element(s). We also analyzed resin-embedded natural sediments for comparison of LA-ICP-MS line-scan data to parallel sub-samples measured by SN-ICP-OES and SN-ICP-MS. In general, the results from LA-ICP-MS line-scans of natural sediments correspond well with reference values and with high reproducibility, corroborating the results of the artificial laminations. The results for Ca, V, Mn, Sr, Mo, Ba, and U (in log-ratios to Al) suggest that these elements can be analyzed semi-quantitatively, showing correlation coefficients (R^2) ranging from 0.59 to 0.85 compared to conventional analytical techniques. However, we show that using non-matrix matched calibration standards such as NIST SRM 610 may induce deviations from the LA-ICP-MS values to the reference values. Consequently, we recommend a simple protocol for further data correction in which binned-mean LA-ICP-MS values are calibrated to a parallel series of discrete samples analyzed by these conventional techniques.

1. Introduction

Laser ablation-inductively coupled plasma-mass spectrometry (LA-ICP-MS) has become a widely accepted analytical tool for geological samples, but also for samples in many other research fields (see Durrant and Ward, 2005). LA-ICP-MS measurements show generally low detection limits, high accuracy, reasonable precision, and linear calibration graphs over several orders of magnitude and at high spatial

* Corresponding author. Tel.: +31 0302535004.
E-mail address: rick.hennekam@nioz.nl (R. Hennekam).
[1] Current address: Geology Department, Royal Netherlands Institute for Sea Research (NIOZ), 1797 SZ Den Hoorn (Texel), The Netherlands.

http://dx.doi.org/10.1016/j.chemgeo.2015.03.004
0009-2541/

resolution (μm-scales) (e.g. Perkins et al., 1991, 1993; Jarvis and Williams, 1993; Günther et al., 1998). These analytical capabilities also make LA-ICP-MS potentially very suitable for detailed line-scan sampling across sample surfaces (Jarvis and Williams, 1993) such as laminated sediments.

Laminated (varved) sediments provide one of the highest possible temporal resolutions for establishing detailed paleoclimate records (Pike and Kemp, 1996). Unfortunately these sediments are frequently unconsolidated and sampling them while preserving the laminations can be cumbersome. Fluid-displacive resin embedding has been established as an adequate method to preserve the laminated structure of the sediment (Pike and Kemp, 1996; Lotter and Lemcke, 1999; Jilbert et al., 2008). An auxiliary benefit of resin embedding is that samples can be directly measured by LA-ICP-MS line-scanning (Jilbert et al., 2008). This method has been successfully applied to reconstruct past variability in the marine environment (e.g. Jilbert et al., 2010; Jilbert and Slomp, 2013; Lenz et al., 2014).

Many studies have discussed the difficulties of quantitative analysis by LA-ICP-MS on more homogenous materials, with the principal limitation being elemental fractionation (e.g. Fryer et al., 1995; Günther et al., 1997; Mank and Mason, 1999; Guillong and Günther, 2002; Kroslakova and Günther, 2007). Elemental fractionation in LA-ICP-MS analyses is caused by: (1) non-stoichiometric sampling by the laser (Cromwell and Arrowsmith, 1995; Eggins et al., 1998), (2) selective transport of aerosols formed during the laser ablation (Cromwell and Arrowsmith, 1995; Košler et al., 2005), and (3) incomplete vaporization/atomization/ionization of the aerosols within the ICP (Kroslakova and Günther, 2007). These effects are minimized when the matrix of the calibration standard is similar to the matrix of the analyte. Laminations however can consist of the repeated alternation of potentially rather different matrices. Therefore, this impact on analytical accuracy and precision during LA-ICP-MS line-scan measurements needs to be established.

This study aims to test the accuracy and precision of LA-ICP-MS for geochemical analyses of resin-embedded sediments, with a focus on line-scan analysis, by measurement of samples with a known composition. The study is divided into three sections. Firstly, we prepared and analyzed resin-impregnated homogenized samples ('standards'), consisting of commonly occurring sediment matrices spiked with selected elements. We compare data by LA-ICP-MS to those by conventional techniques, across a range of concentrations. Secondly, we produced synthetic resin-embedded laminated sediments using the spiked sediments to explore accuracy and precision of LA-ICP-MS line-scanning on sub-mm spatial scales. Thirdly, we expanded the study to investigate a wider range of elements in natural sediments. Specifically, we investigated potential artifacts induced by using a non-matrix matched calibration standard (NIST SRM 610 glass). For this purpose, trace metal-rich sediments from the Levantine Basin in the eastern Mediterranean were resin-embedded and analyzed by LA-ICP-MS. These LA-ICP-MS line-scan measurements were compared to those on parallel sub-samples measured with conventional analytical techniques.

2. Material and methods

2.1. Resin-embedded standards: homogenized pellets

We selected calcite, quartz, and clay (aluminosilicates) as matrices for a series of resin-embedded homogenized pellet standards. Specifically, calcite ($CaCO_3$; Merck Millipore, 99.95 Suprapur) and quartz (SiO_2; Merck Millipore) were used, while a finely ground montmorillonite ($(Na,Ca)_{0.33}(Al,Mg)_2(Si_4O_{10})(OH)_2 \cdot nH_2O$) sample was used as a pure clay end-member. For spiking of the sedimentological matrices, a standard-addition matrix (SAM) was prepared. This SAM consists of a mixture of powders: V_2O_5, MoS_2, $BaCO_3$, and Al_2O_3. These powders were added in weight ratios of 1:1:10:100, of V, Mo, Ba, and Al respectively. We focused on these four elements to keep the spiked standards relatively simple in terms of their matrix, while including a wide atomic mass range to allow recognition of mass-induced biases if present. Moreover, in paleoclimatic studies these elements are commonly used as redox indicator (V and Mo) and as an export-productivity proxy (Ba) (e.g. Jilbert et al., 2010). The sedimentological matrices and the SAM were ground separately in an automated mill at least three times (for quartz, six times), in order to obtain a sufficiently small grain size (≤1 μm) for LA-ICP-MS analysis and mix the individual compounds of the SAM mixture.

Subsequently, the SAM was added to the sediment matrices in ten different quantities. This produced a set of thirty standards with a range of concentrations (Table S1 of the Supplementary material). For homogenization purposes all thirty standards were milled again three times.

A homogenized pellet of each standard was then embedded in epoxy resin. For embedding we used the low viscous Spurr Epoxy Resin, which usually results in good impregnation of sediments (Pike and Kemp, 1996; Lotter and Lemcke, 1999; Jilbert et al., 2008) and contains negligible metal concentrations (Shaheen and Fryer, 2011). Perspex blocks (dimensions: ~50 mm × ~30 mm × ~1.5 mm) with ten holes were used as recipients for the standards. For each of the three matrices the ten standards were put in one of these Perspex blocks, which were closed at the bottom using tape (Fig. 1; Step 1A). Subsequently, the standards were embedded in a vacuum chamber for optimal infiltration of the resin. The resin was released from a syringe by the use of a three-way valve connected to the vacuum chamber (Fig. 1; Step 2A). Tape was used to retain the resin on top of the standards (Fig. 1; Step 3A). After applying the resin, the samples were left for 48 h before curing them in an oven at 60 °C for 48 h. After a mild abrasion and polishing of the surface at the bottom of the Perspex blocks (Fig. 1; Step 4A) the polished surfaces of those standards were used for LA-ICP-MS analyses.

2.2. Resin-embedded standards: synthetic laminations

Synthetically laminated sediment standards were prepared in a small plastic vessel. First, a selected powder standard (Table 1) was spread over the surface of the vessel, resin-embedded in the vacuum chamber, left for 48 h, and cured in an oven (Fig. 1; Steps 1B–3B). After abrasion and polishing of the sample, a resin-embedded block was produced of a single (spiked) matrix. A microdrill was used to form a sequence of grooves in the resin block (Fig. 1; Step 4B). The first three steps were then repeated with another selected sediment standard (Table 1) to fill-up the grooves, forming the artificial laminations (Fig. 1; Steps 1B–3B repeated). These synthetic laminations were revealed subsequently after careful abrasion and polishing (Fig. 1; Step 5B). We prepared two synthetically laminated standards: (1) a sequence of laminations with the same matrix (calcite), but an order of magnitude difference in SAM concentrations, and (2) a sequence of laminations with a different matrix (calcite and quartz), but similar SAM concentrations (the used spiked sediments are indicated in Table S1 of the Supplementary material).

2.3. Resin-embedded eastern Mediterranean sediments

Aluminum trays of 20 cm length were used to sample sediments from an open piston core (MS21PC; 32°20.7′N, 31°39.0′E; 1022 m depth) from the eastern Mediterranean Sea. We focused on the interval of an organic-rich layer (sapropel S1), which is generally known to contain a well-preserved sapropel, enriched in trace metals (e.g. Warning and Brumsack, 2000). The samples in the aluminum trays were resin-embedded through a deionized water–acetone–epoxy resin-exchange procedure in an argon-filled glove box for redox-sensitive element preservation (see for details Jilbert et al., 2008). The resin-embedded

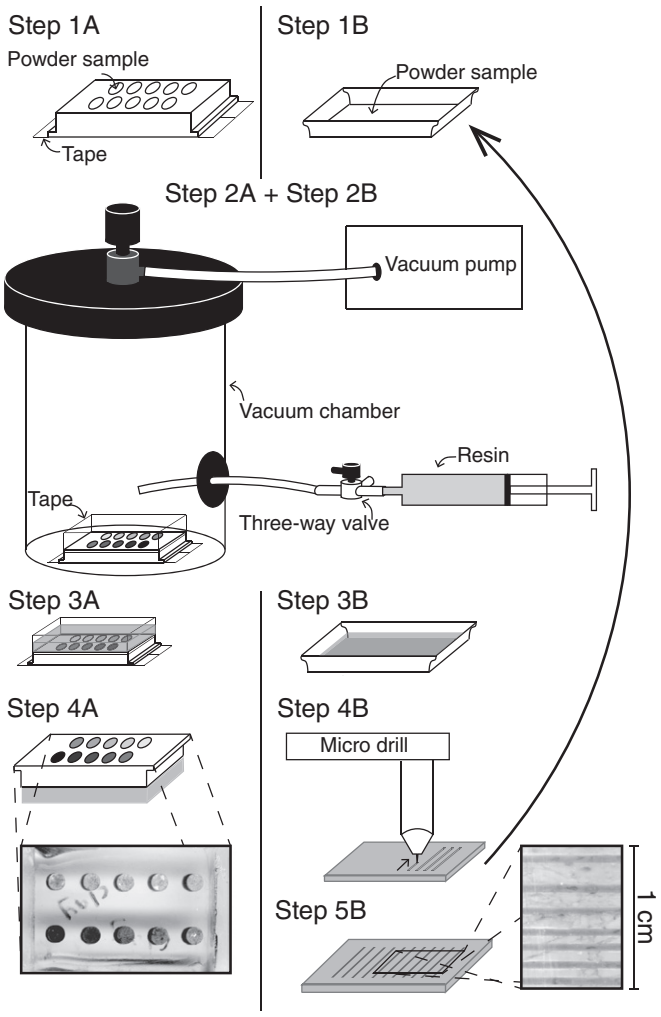

Fig. 1. Steps involved in the production of resin-embedded homogenized pellet standards (Steps 1A–4A) and production of resin embedded synthetically laminated standards (Steps 1B–5B). Details are given in Sections 2.1 and 2.2.

sediment was cut perpendicular to the sedimentation plane, then cut to form blocks that fit the ablation chamber (~5 cm), and polished.

Several blocks were selected for further LA-ICP-MS line-scan analysis. Selection was done to capture (parts of) the trace metal excursions during sapropel formation observed for discrete (0.5-cm) samples from the same depth-interval. The latter measurements were done by conventional bulk geochemical techniques: solution nebulization-ICP-optical emission spectroscopy (SN-ICP-OES) and SN-ICP-MS. To directly compare methods, 0.5-cm binned means of the equivalent depth-intervals for the LA-ICP-MS measurements were calculated.

2.4. LA-ICP-MS measurements and processing

A 193 nm wavelength COMPex 102 ArF excimer laser ablation system (Lambda Physik, Göttingen, Germany) connected to an Element 2 sector field ICP-MS (Thermo Scientific, Bremen, Germany) was used for all LA-ICP-MS analyses at the University of Utrecht. The use of a deep ultra-violet (193 nm) laser beam has been proven to significantly reduce elemental fractionation effects during the ablation process compared to infrared lasers (Günther et al., 1997). The ICP-MS was operated at low resolution ($M/\Delta M = 400$), to provide optimal detection capability and sensitivity of the ICP-MS, with a relatively high measurement frequency during line-scan analyses. The measurement frequency of the ICP-MS for all isotope spectra of this study was ~2.5–3 Hz.

Samples were placed into a He-flushed ablation chamber for LA-ICP-MS analysis. For line-scanning the ablation chamber was moved perpendicular to the (synthetic) laminations of the resin-embedded sediment samples, commonly at a speed of 0.0275 mm s^{-1}. In general the laser parameters were kept constant at a pulse repetition rate of 10 Hz, spot diameter of 80 μm, and energy density of ~8 J cm^{-2}. Laser input at the ablation site (fluence) was monitored daily before tuning the ICP-MS for optimal sensitivity following the procedure of Wang et al. (2006). The measurement frequency and scanning rate (i.e. movement speed of the stage) resulted in a constant shift increment of ~10 μm per measurement (i.e. an ICP-MS cycle of all elements). When added to the laser spot diameter, this resulted in an overall sampled interval of ~90 μm per ICP-MS cycle, with an 80 μm overlap with the previous and subsequent measurement. Typical ICP-MS and laser settings are indicated in Table 1. We optimized these settings through testing of variable pulse repetition, spot diameter, and scanning rate (Supplementary material, Fig. S1).

LA-ICP-MS data were processed following the procedure of Longerich et al. (1996). In short, the mean background values were obtained from the mean of intensities of an ~30 s interval before the start of the laser ablation measurement. These values were subtracted from the raw analyte intensities. The sensitivities of the isotopes (in this study relative to ^{27}Al) were calculated by measurement of an external standard (NIST SRM 610). Subsequently the background-corrected analyte intensities were corrected for the relative sensitivity of the specific isotope and its natural abundance. NIST SRM 610 reference values were

Table 1
Typical LA-ICP-MS settings for measurements on resin embedded samples.

ICP-MS type	Thermo Scientific Element 2
RF power	1300 W
Plasma gas	Ar (16.00 l min^{-1})
Auxiliary gas	Ar (0.85 l min^{-1})
Carrier gas	Ar (0.67 l min^{-1}) and He (0.75 l min^{-1})
Skimmer cone	Aluminum
Sampler cone	Nickel
Measurement frequency	~2.5–3 Hz
Resolution	Low (M/ΔM = 400)
Isotopes	^{27}Al, ^{29}Si, ^{44}Ca, ^{51}V, ^{55}Mn, ^{65}Cu, ^{66}Zn, ^{88}Sr, ^{97}Mo, ^{137}Ba, ^{238}U
Laser type	COMPex 102 (ArF Excimer, Lambda Physik)
Wavelength	193 nm
Fluence	8 J cm^{-2}
Spot size diameter	80 μm
Repetition rate	10 Hz
Scanning rate	0.0275 mm s^{-1}

taken from Jochum et al. (2011), while the natural abundances of the isotopes were taken from Berglund and Wieser (2011). Because the yield of ablated material varies during LA-ICP-MS, data are commonly reported as ratios of the analyte element to an internal standard. In our resin-embedded homogenized pellets the internal standard was Ca, Si, or Al, depending on the matrix (respectively calcite, quartz, clay). For the resin-embedded synthetically laminated sediments the internal standard was Ca for the sequence of laminations with a calcite matrix, while Al was used for the sequence of laminations consisting of an alternation of calcite and quartz. We prefer to present the data as ratios because on μm- to mm-scales no internal standard with a known concentration is available during LA-ICP-MS line-scanning of natural samples. We report log-ratios to avoid the asymmetrical properties of normal ratios (Aitchison and Egozcue, 2005). Log-ratios are, therefore, more suitable for multivariate statistics and calibration, as shown in an earlier core scanning study by X-Ray Fluorescence (XRF) analysis (Weltje and Tjallingii, 2008).

In order to report precision (relative standard deviation, RSD) of the LA-ICP-MS measurements of the resin-embedded homogenized pellet samples, we repeated spot analyses three times at different sites for the same standard material. For line-scan analyses of the synthetic laminations the precision was based on the RSD of the LA-ICP-MS measurements within a spatial interval of line-scanning on the same spiked matrix. These spatial intervals are clearly indicated in the relevant figures. Accuracies of the analyses are reported as deviations (in absolute percentages) of the LA-ICP-MS log-ratio values to the reference log-ratio values.

2.5. Bulk geochemical measurements: SN-ICP-MS, SN-ICP-OES, and XRF-bead

Subsamples from all standard powders after the addition of the SAM and homogenization were measured by more traditional techniques: SN-ICP-OES, SN-ICP-MS, and XRF analysis on glass beads (XRF-bead). This was done to assess contamination during the milling stage (Durrant, 1992), and to provide reference data for the LA-ICP-MS study.

Before analyses by SN-ICP-OES and SN-ICP-MS, aliquots of all thirty produced spiked sediment standards were totally digested (following Reitz et al., 2006). Approximately 125 mg of sample was digested in a Teflon vessel using HF and an $HClO_4$–HNO_3 mixture. The vessels were closed and left overnight on a hot plate at 90 °C. Samples were then dried on a hot plate at 160 °C. During this step Si is lost, as it forms a SiF_4 azeotrope with water. Thereafter, 25 ml of ~1 M HNO_3 was added and the closed vessels were left on a hot plate at 90 °C for another night. All samples were subsequently measured for major and minor elements with a Spectro Ciros Vision ICP-OES at Utrecht University. Each series of samples contained at least two blanks and two reference samples (international soil sample ISE 921; Van Dijk and Houba, 2000). After ICP-OES measurements, the samples were further diluted to measure major, minor, and trace element compositions with a Thermo Scientific X-Series 2 ICP-MS at Utrecht University. Analytical precision and accuracy for both techniques were better than 5% for the target elements (Al, V, Mo, and Ba).

The sediment standards were also measured by XRF analysis on fused glass beads. Preparation and analysis with a Philips PW 2400 X-ray spectrometer were done at the Institute of Chemistry and Biology of the Marine Environment (ICBM) in Oldenburg, Germany. The protocol of Schnetger et al. (2000) was used for the preparation of the fused glass beads by mixing ~700 mg of sample with 4200 mg $Li_2B_2O_7$, and pre-oxidation at 500 °C with NH_4NO_3. Replicate analyses of in-house standards and international reference standards show that the precision and accuracy of the measurement were better than 6% for the target elements. For one of the artificial standards (quartz; ~5000 μg g^{-1} added Al; see Table S1 in Supplementary material) insufficient material was present for an XRF-bead measurement.

The eastern Mediterranean sediment samples were also measured by SN-ICP-OES and SN-ICP-MS following the same procedures as above. For the SN-ICP-OES measurements all samples were measured with a 0.5-cm resolution. In addition, a selection of samples (~2-cm resolution) was measured by SN-ICP-MS. For some SN-ICP-OES measurements, in the eastern Mediterranean sediment samples, Mo values were below detection limit. Consequently, in these samples, we only use SN-ICP-MS measurements for Mo calibration against the LA-ICP-MS measurements.

3. Results and discussion

3.1. Reference values for LA-ICP-MS analyses

The measurements of the spiked artificial sediment standards by traditional analytical methods (SN-ICP-OES, SN-ICP-MS, and XRF-bead) show similar results (Table S1 of the Supplementary material) that lie predominantly within their respective uncertainty intervals. Some offsets in accuracy were observed between analyses and the intended standard addition values, in part due to the natural occurrence of elements in the matrices (e.g. Al and Ba in clay). Offsets of other elements could be due to contamination or selective removal of components during milling as a result of adherence to the walls of the mill. Nevertheless, because the results of the conventional analyses are similar within analytical uncertainty, we consider these values to be reliable and henceforth use averages of these values as benchmark values for comparison with the LA-ICP-MS analyses (Supplementary material, Table S1).

3.2. Homogenized pellet standards

3.2.1. LA-ICP-MS on resin-embedded homogenized pellet standards

LA-ICP-MS spot analyses of the resin-embedded sediment standards are compared to their reference log-ratio values in Fig. 2. The standards with a calcite matrix show good accuracy and high precision with linear regressions close to $y = x$ and R^2 values of 1.00. Deviations of the LA-ICP-MS-based values from the reference values never exceed 3%. Triplicate LA-ICP-MS analyses show high internal consistency with mean RSDs below 3% for all elemental log-ratios.

Similarly, the LA-ICP-MS measurements of the quartz matrix-based standards show linear correlations with high correlation coefficients to their reference values. The log-ratios of the LA-ICP-MS measurements lie on average within 6% of the reference values for V/Si, Mo/Si, and Ba/Si, and within 12% for Al/Si. The mean RSDs are below 3% for all elemental log-ratios.

For the clay (montmorillonite) matrix, V/Al and Mo/Al also show linear correlations with high correlation coefficients, with on average LA-ICP-MS values within 3% of the reference values, and mean RSDs <1%.

However, for Si/Al and Ba/Al the mean deviations from the reference values are relatively large, at ~43% for Si/Al and ~15% for Ba/Al. The reproducibility of the LA-ICP-MS log-ratios of Si/Al and Ba/Al is respectively <15% and <4%. The regressions indicate linear behavior with high R^2 values for Si/Al and Ba/Al, but with deviating slopes (from $y = x$) of respectively ~0.8 and ~1.2.

3.2.2. Inter-matrix comparison and deviant behavior of Si/Al in the clay matrix

Milling appears to have contaminated some standards (e.g. minor amounts of Ca are present in quartz standards, and Si in calcite standards, see Supplementary material, Table S1). One benefit of this contamination is that the spiked sediment standards contain a measurable amount of each element in all samples. This allows log-ratios of the elements (Si/Al, Ca/Al, V/Al, Mo/Al, and Ba/Al) to be plotted for each standard (Fig. 3). The log-ratios to Al for V, Mo, Si, and Ca show linear correlation with high accuracy over several orders of magnitude, independent of the matrix. Interestingly the Si/Al of the clay standard seems to fit well to this linear regression, despite the apparently poor fit when the clay-standards are plotted alone (Fig. 2). This might indicate that the low range of log-ratios of Si/Al in the clay standards (0 to 0.5) is insufficient to demonstrate a proper linear regression, observed across a wider range of concentrations. Hence, we regard our LA-ICP-MS results for Si/Al of the clay-based resin-embedded homogenized pellet standards as tentative, until tested across a wider concentration range.

3.2.3. Deviant behavior of Ba/Al in the clay matrix: influence of variable chemical phases?

In the spiked clay standards Ba is present in (at least) two phases: (1) Ba related to the aluminosilicates (henceforth Ba-clay) evidenced by high Ba values in the un-spiked clay standards, and (2) $BaCO_3$ artificially added for spiking of the standards. Barium (in a log-ratio to Al) shows its largest deviation against the 1:1 line for the standards with only minor addition of $BaCO_3$, which implies that most Ba is present as Ba-clay. After several standard addition steps the $BaCO_3$–Ba contribution exceeds that of Ba-clay, leading to lower deviation from the reference values. We speculate that the relative sensitivity of Ba under LA-ICP-MS (measured intensities per concentration) differs between the two compounds. Therefore, depending on the relative proportion of either of the two phases, elemental fractionation during LA-ICP-MS sampling can lead to variability in the Ba/Al values as observed in Figs. 2 and 3.

To further test this hypothesis we modeled the theoretical Ba/Al ratio of the spiked clay standards using different sensitivities of Ba-clay and $BaCO_3$ (Fig. 3b). For this purpose we assumed the Ba related to the aluminosilicates to be ~1500 ppm (based on the reference value of the pure clay samples) and calculated the relative proportions of Ba-clay and $BaCO_3$ in each standard. We then adjusted the relative sensitivity of Ba-clay to obtain log(Ba/Al) closest to the reference values ($y \approx x$). This yielded a relative sensitivity (concentration/LA-ICP-MS intensity) for Ba-clay of ~1.52 higher than the sensitivity obtained by NIST SRM 610, implying that for Ba-clay a specific LA-ICP-MS yield relates to a higher Ba concentration compared to NIST SRM 610 or $BaCO_3$. The

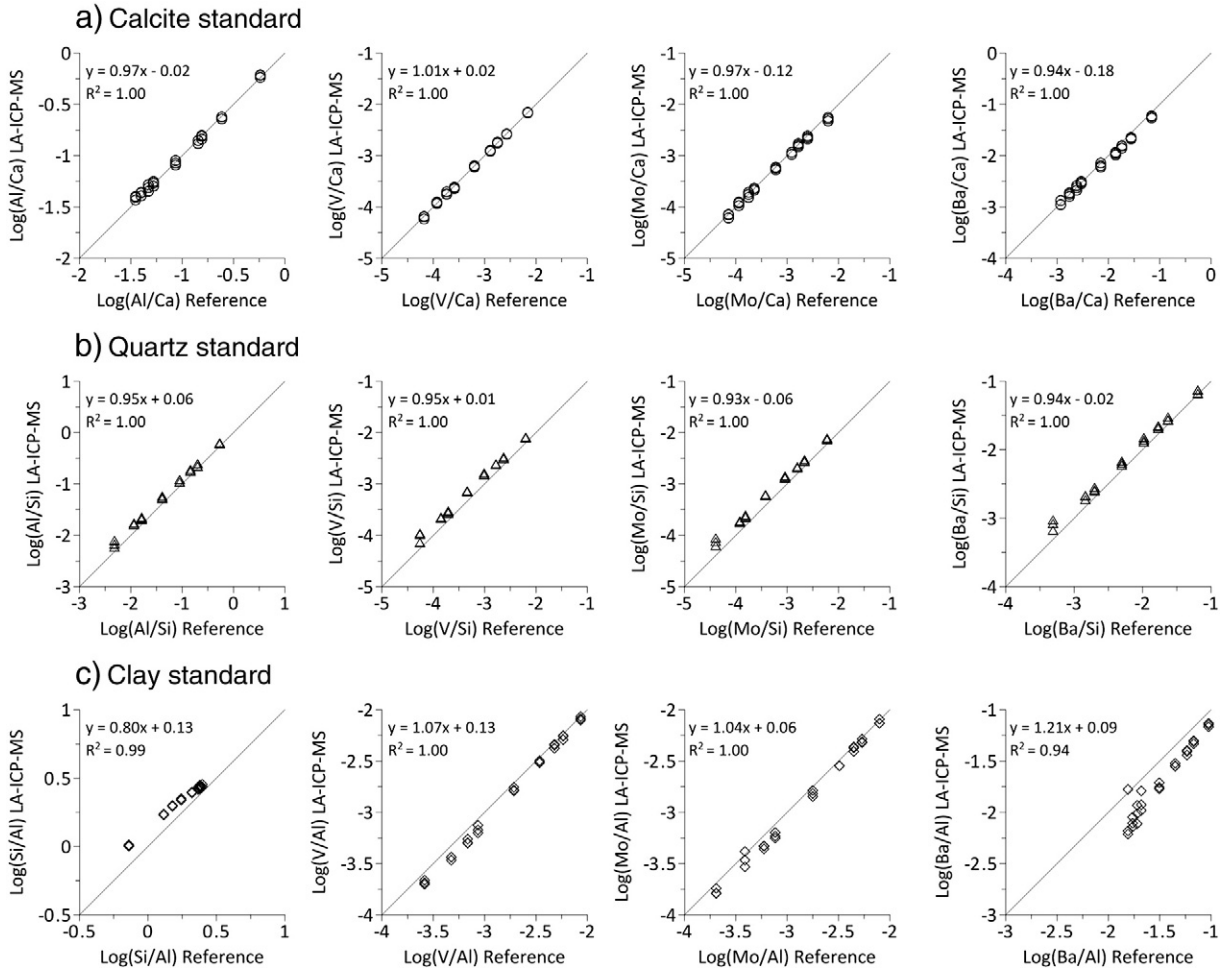

Fig. 2. Plots of LA-ICP-MS spot analyses on the resin embedded homogenized-pellet standards to their reference values. Log-ratios of target elements are shown with Ca, Si, and Al as denominators for respectively the calcite (a), quartz (b), and clay (c) standards. 1:1 correlation lines are also plotted.

resulting log(Ba/Al) model shows increased accuracy for the values of the clay-based standards (Fig. 3b). The modeled Ba/Al in the clay standards shows some remaining offsets compared to the spiked calcite- and quartz-based standards, hence the influence of sample matrix on estimated values of Ba/Al cannot be excluded.

Variable sensitivities for Ba-clay and $BaCO_3$ were not observed for the conventional SN-ICP-MS measurements (Table 1), and thus we conclude that these effects are laser induced. Elemental fractionation during LA-ICP-MS may principally occur during aerosol formation, aerosol transport, and/or aerosol interaction with the ICP (see Pisonero et al., 2009 and references therein). Possibly the Ba-clay and $BaCO_3$ form different aerosols during laser ablation that subsequently behave differently during transport to the ICP and/or in the plasma of the ICP. The low second ionization energy of Ba potentially results in a relatively large production of doubly charged Ba ions in the ICP (e.g. Gray and Williams, 1987), which could also affect the amount of Ba^+ detected in the MS at m/z 137 and 138, if aerosol dependent.

3.3. Resin-embedded synthetically laminated standards

3.3.1. LA-ICP-MS analyses of the synthetic laminations

LA-ICP-MS line-scanning of the synthetic laminated sediments was performed for five laminae 'couplets' over ~7.5 mm. We investigated standards consisting of synthetic calcite laminations (Fig. 4a) and those with alternating calcite and quartz laminations (Fig. 4b), focusing on two of those couplets (Fig. 4; see Supplementary material, Fig. S1 for full profiles). The dotted lines on the figure indicate the expected 'theoretical' reference values for these laminations, which are evident from their geochemical signature.

The laser scans of the laminations follow the reference values for all elemental log-ratios. Most elemental log-ratios show minor deviations (generally <5%) from the reference values and low RSDs (generally <5%) (Fig. 4).

The transition between two consecutive layers of different compositions leads to a mixing zone of the geochemical signals of those layers during line-scanning. At ~10 μm shift increment per measurements and 80 μm spot size of the laser this mixing zone should theoretically involve ~8 measurements. For most elements this mixing zone is indeed observed to involve 8–10 measurements as expected (Fig. 4).

The log-ratio of Ca/Al in the synthetically laminated standard containing calcite and quartz laminae shows a clear tailing signal at the transition from the layer with mainly a calcite matrix (Ca ≈ 350,000 ppm) to the quartz-matrix lamination (Ca ≈ 1200 ppm) (Fig. 4b). Such memory effects are not observed for Si, Ba, and V. However, for these elements, relatively high concentrations are maintained in all laminations, which may limit these tailing effects. For all elements unreliable data may occur at transitions from a lamination enriched in an element to a lamination devoid (i.e. close to detection limit) of an element. This kind of memory effect is suspected to be due to re-suspension of material (in this case Ca-rich material) at the sample surface itself, in the transfer line, and/or in the ablation chamber (Mason and Mank, 2001). It may also be due to deposition/re-suspension in the ICP-MS system, e.g. at the sampler and skimmer cones (Jenner et al., 1990). Sample chamber design is known to influence flush-out time of the ablation aerosols (Gurevich and Hergenroder, 2007), so these memory effects can possibly be reduced by optimizing sample cell geometry.

To investigate the effects of porosity on the LA-ICP-MS line-scan analyses, the calcite matrix was line-scanned in an interval with visibly variable resin content (Fig. 5; only shown for log-ratio of Ca to Al). The high variation of raw ^{44}Ca counts indicates that the proportion of resin to sediment sample was variable. There is no strong variability observed in log(Ca/Al) relative to the reference values, despite this large variability in porosity. Moreover, there is no correlation between the deviation from the reference value and the ^{44}Ca intensities. Similarly, for the log-ratios of V/Ca, Mo/Ca, and Ba/Ca, there is no correlation between the amount of material blated and deviation from the reference values (R^2

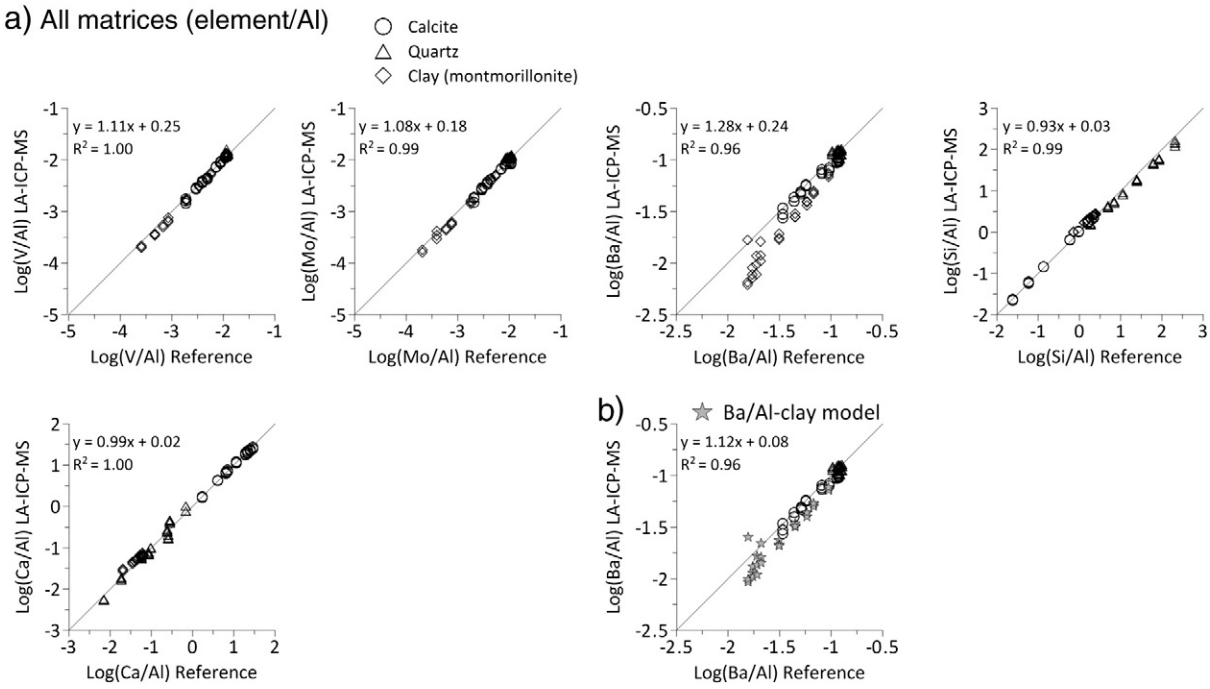

Fig. 3. (a) Plots of LA-ICP-MS spot analyses on the resin embedded homogenized-pellet standards to their reference values for all matrices combined. Log-ratios of target elements are shown with Al as a denominator for all matrices. 1:1 correlation lines are also plotted. (b) Plot of log(Ba/Al) produced by LA-ICP-MS spot analyses on the resin embedded homogenized-pellet standards to their reference values for all matrices, but with different relative sensitivities assigned to Ba-clay in the clay standards (i.e. Ba/Al-clay model). See Section 3.2.3 for details.

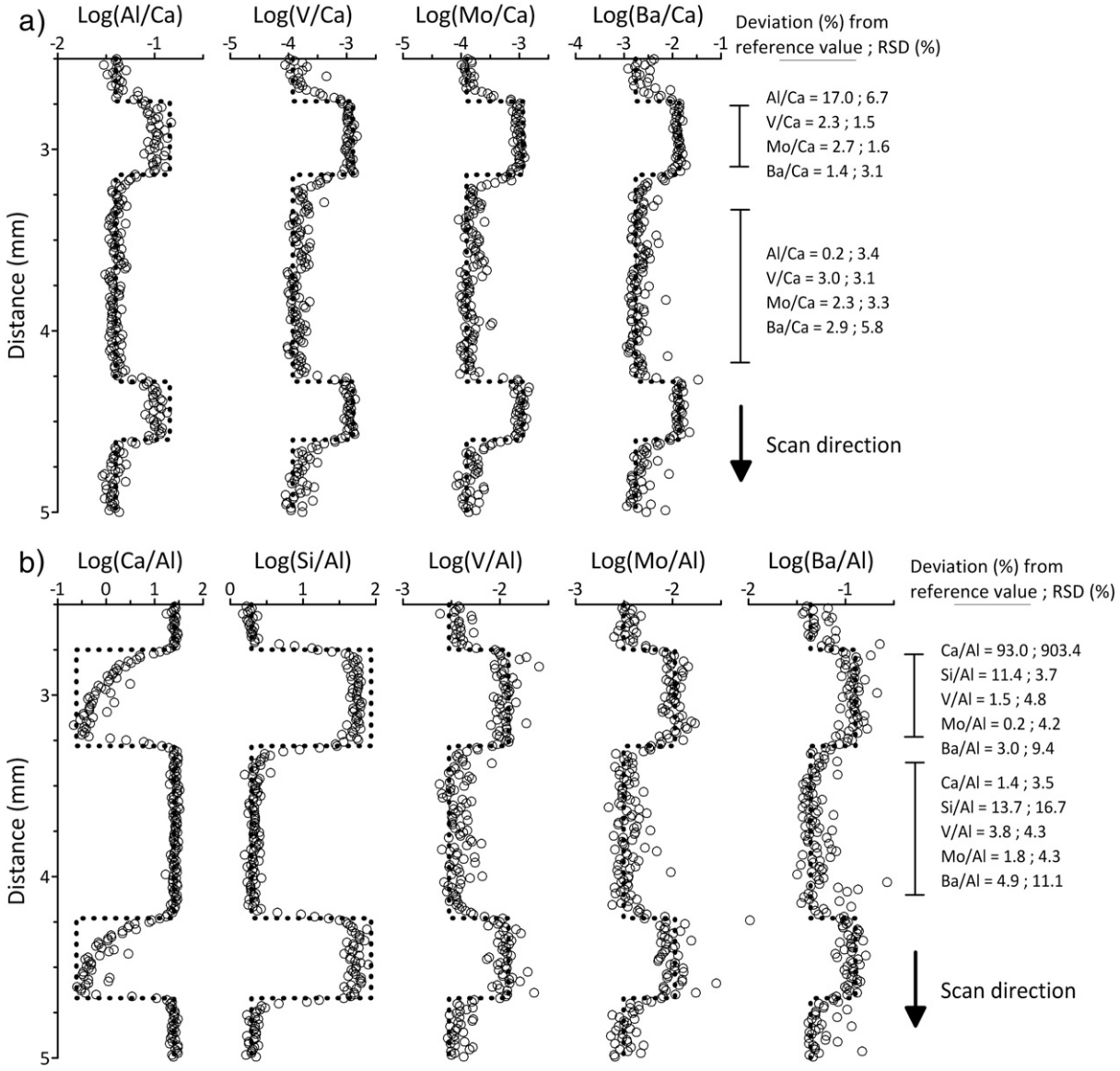

Fig. 4. LA-ICP-MS line-scan profiles of two representative laminations in the synthetically laminated standards. (a) Sequence of synthetic laminations with the same matrix (calcite), but an order of magnitude difference in SAM concentrations (log-ratios to Ca). (b) Sequence of synthetic laminations with a different matrix (calcite and quartz), but similar SAM concentrations (log-ratios to Al). Dotted lines indicate the theoretical reference values for the laminated standards. The deviations from the reference values and relative standard deviations are given. Line-scan direction (top to bottom) is indicated.

ranging between 0 and 0.02). This indicates that porosity does not affect the LA-ICP-MS line-scan measurements in our samples.

3.4. LA-ICP-MS data in natural sediment samples

3.4.1. LA-ICP-MS line scan analysis in natural sediment samples: V/Al, Mo/Al, and Ba/Al

The resin-embedded and LA-ICP-MS line-scanned sediments from the eastern Mediterranean sapropel show log-ratio profiles for V/Al, Mo/Al, and Ba/Al that are similar as those from conventional analytical techniques (Fig. 6), confirming that the elements in these ratios may be reliably measured by LA-ICP-MS. The binned means of the LA-ICP-MS measurements show similar linear correlations to these reference values with relatively high R^2 values (Fig. 6b). Table 2 shows that for V/Al, Mo/Al, and Ba/Al the mean deviations from reference values are respectively <3, <8, and <4%, with mean RSDs <2% for all these elements.

Despite the good agreement between the LA-ICP-MS values to 'reference' values, the log-ratios of V, Mo, and Ba to Al were systematically lower in the LA-ICP-MS measurements (Fig. 6a, b). These results suggest that complex matrices, such as encountered in actual sediments, may influence the fractionation of elements during LA-ICP-MS, creating a net sensitivity for each element which may differ from that in the glass standard NIST SRM 610. Alternatively, some common elemental phases in real sediments may exhibit intrinsic sensitivities, which differ from those observed in the glass standard, as seen for the Ba-clay component in the homogenized-pellet standards. The possible causes of these elemental fractionation effects are largely unknown, but seem related to particle generation by laser ablation (see Section 3.2.3) and may be diminished by using matrix-matched standards (e.g. Mank and Mason, 1999; Kuhn and Gunther, 2004; Košler et al., 2005; Liu et al., 2008).

Deviation of resin-embedded natural sediment sensitivities from glass standard sensitivities has also been observed for Mo/Al in Baltic Sea sediments (Jilbert and Slomp, 2013). Fig. 7 shows the log(Mo/Al) calibration for LA-ICP-MS and SN-ICP-OES data of these Baltic Sea samples (Jilbert and Slomp, 2013), plotted together with our log(Mo/Al) data from Mediterranean samples. The Mo/Al values of the Baltic

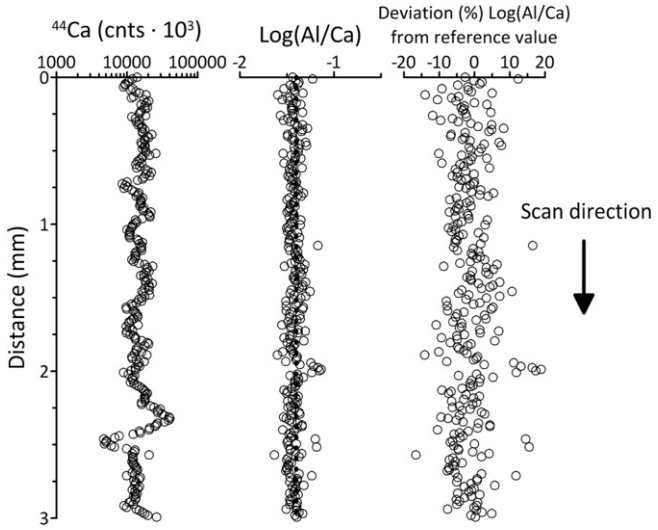

Fig. 5. LA-ICP-MS line-scan profile of raw ^{44}Ca intensities, log(Al/Ca) values, and the deviation of the log(Al/Ca) from the reference value, to determine the effects of porosity differences. Dotted line indicates the theoretical reference values for log(Al/Ca).

samples are generally higher than the 1:1 line (on average 7%), while the Mediterranean samples are generally lower than the 1:1 line (on average 7%). All LA-ICP-MS measurements were done with exactly the same instrumental set-up and similar ablation conditions at Utrecht University. Assuming the Mo phases to be similar between the two sediments (precipitated under anoxic conditions), and SN-ICP-OES and SN-ICP-MS measurements are accurate (we also show SN-ICP-OES values for the Mediterranean samples in Fig. 7 being similar to the SN-ICP-MS values), these mismatches must be caused by differences in matrix between samples from different locations. Variations in absolute element abundances could thus reflect matrix differences rather than real concentration changes. However, in this example, these matrix effects may only explain a relatively minor part (~14%) of the variability in the log-ratio of Mo to Al (Fig. 7).

3.4.2. LA-ICP-MS line scan analysis in natural sediment samples: other elemental ratios

Table 2 shows the LA-ICP-MS line-scan results for a selection of elements in sapropel sediments from the eastern Mediterranean. Mn, Sr, and U (in log-ratios to Al) show well-defined linear calibration lines between LA-ICP-MS and reference data, with high R^2 values, low deviation from reference values and good reproducibilities. Log(Ca/Al) correlates

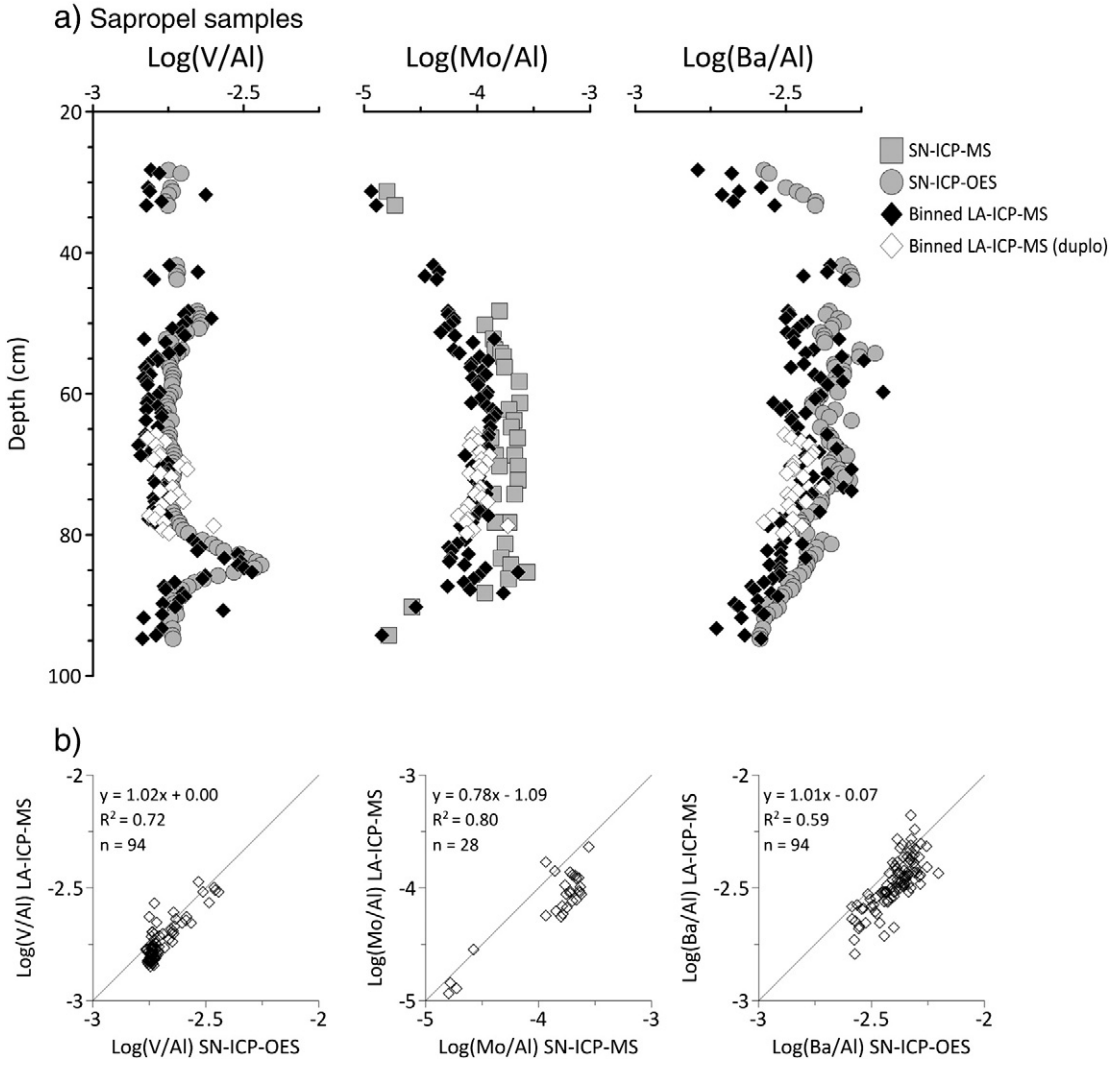

Fig. 6. (a) Log-ratio profiles for V, Mo, and Ba to Al for eastern Mediterranean sapropel sediment samples. Binned mean LA-ICP-MS line-scan values were calculated for direct comparison to SN-ICP-OES or SN-ICP-MS results. (b) Plots of SN-ICP-OES/SN-ICP-MS values to binned mean LA-ICP-MS values. 1:1 correlation lines are plotted.

Table 2
Summary of the statistical data produced by comparison of binned mean values from LA-ICP-MS line-scanning to reference methods for a selection of elemental log-ratios. The absolute deviations from the reference values were used to calculate the mean deviations.

Element (log-ratio)	Linear equation	R^2	Mean deviation (%) from reference value	Mean RSD (%)	Reference method
Ca/Al	$y = 1.02x - 0.13$	0.65	70.86	14.00	SN-ICP-OES
V/Al	$y = 1.02x + 0.00$	0.72	2.05	1.20	SN-ICP-OES
Mn/Al	$y = 0.83x - 0.50$	0.83	8.01	1.00	SN-ICP-OES
Cu/Al	$y = 1.16x + 0.62$	0.16	3.83	1.59	SN-ICP-OES
Zn/Al	$y = 0.33x - 2.14$	0.05	7.15	1.24	SN-ICP-OES
Sr/Al	$y = 0.93x - 0.28$	0.64	5.68	1.68	SN-ICP-OES
Mo/Al	$y = 0.78x - 1.09$	0.80	7.26	1.62	SN-ICP-MS
Ba/Al	$y = 1.01x - 0.07$	0.59	3.90	1.87	SN-ICP-OES
U/Al	$y = 1.07x + 0.08$	0.85	5.01	0.84	SN-ICP-MS

well with the reference values but displays higher deviation, potentially due to the occurrence of calcite tests in this interval. Log(Cu/Al) shows low deviation from the reference value over the sapropel interval, but also a low R^2 value in the respective calibration equation. This seems to be the result of the narrow range of values for Cu in the samples used. Hence, this element might still show potential for quantitative LA-ICP-MS analysis if further tests across a wider range of concentrations would be carried out. Log(Zn/Al) shows the highest mean deviation from the reference values, and relatively low R^2 values in the calibration equations. Furthermore, the slope of the calibration line is ~0.3 indicating substantially different sensitivity factors for this element between natural sediments and the glass standards. Therefore LA-ICP-MS line-scan data of this element should be interpreted with care.

3.4.3. Data correction procedure for LA-ICP-MS line-scanning of natural sediments

As demonstrated by our homogenized-pellet tests, LA-ICP-MS on resin-embedded sediments shows the calibration lines that are generally linear over several orders of magnitude. Furthermore, for many elements in the matrices tested here, the LA-ICP-MS-estimated values plot close to the 1:1 line with reference data. However, in cases where calibration slopes differ from 1:1, it is necessary to perform a further data correction step on the LA-ICP-MS data. Jilbert and Slomp (2013) used a simple linear regression between a discrete-sample series of bulk-sediment Mo/Al (plotted on the y-axis) and binned means of LA-ICP-MS line-scan data (plotted on the x-axis), to produce plots similar to those in Fig. 2 for selected sediment intervals. The gradient of the calibration line was then used as a multiplier to correct the LA-ICP-MS data for the sediment-specific sensitivity of Mo. This approach seems acceptable if quantitative analyses are desired and no matrix-matched standards are available. We stress that the success of such an extra calibration step is dependent on the relative homogeneity of the matrix through the sequence of laminations and the homogeneity of the main chemical phase of target elements.

4. Conclusions and recommendations

The data presented here indicate that LA-ICP-MS line-scanning has high potential for reliable quantitative analysis of major to trace elements in (laminated) resin-embedded sediments. In general, good accuracy and high precision were shown for V, Mo, Ba, and Al in log-ratios to variable elements (Ca, Si, Al) in both resin-embedded standards (spot analyses) and line-scanned synthetic laminations. We caution that reliable quantitative analysis may be dependent on the matrix and/or the dominant phase of a given element (e.g. Ba in aluminosilicates versus Ba in Ba-carbonate) that is present in the same sample. We observe different relative sensitivities of Ba to Al for these different phases in our LA-ICP-MS analyses for the clay standards. Potentially this can also influence other elements, and this urges further investigations to focus on the implications of varying chemical phases for quantitative analysis in resin-embedded samples. For sediments containing one dominant geochemical phase, reliable semi-quantitative analysis using line-scanning is achievable in a range of common sedimentary matrices.

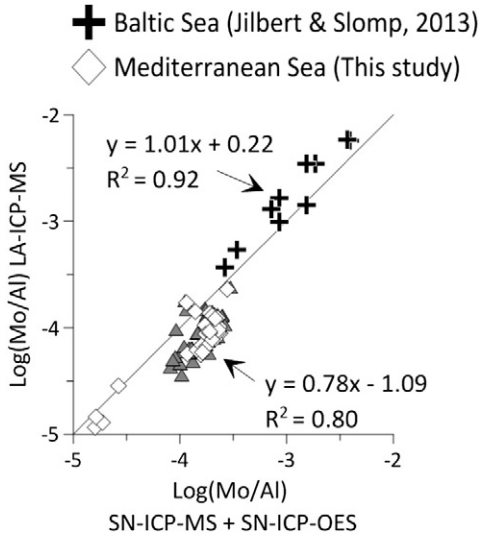

Fig. 7. Plot of binned mean LA-ICP-MS data to conventional data for log-ratio of Mo/Al of eastern Mediterranean samples (this study; SN-ICP-MS; white diamond) to samples from the Baltic Sea (Jilbert and Slomp, 2013; SN-ICP-OES; black plus). Gray triangles indicate the SN-ICP-OES values from the Mediterranean samples, which were under the detection limit for some samples and therefore not used to calculate the linear correlations. The 1:1 correlation line is plotted.

LA-ICP-MS data can be calibrated with conventional techniques such as SN-ICP-OES, SN-ICP-MS, or XRF-bead analyses, which corrects for relative sensitivity offsets between natural sediments and glass standards. By this protocol, (semi-)quantitative estimates of geochemical proxies on (tens of) μm-scales can be produced, allowing high-resolution paleoclimatological and paleoenvironmental reconstructions based on laminated sediments.

Supplementary data to this article can be found online at http://dx.doi.org/10.1016/j.chemgeo.2015.03.004.

Acknowledgments

Two anonymous reviewers and the editor M.E. Böttcher are thanked for constructive comments, which significantly improved the manuscript. At Utrecht University, we thank Helen de Waard and Ton Zalm for analytical assistance with respectively the LA-ICP-MS and the SN-ICP-OES analyses. Erik van Vilsteren and again Helen de Waard are acknowledged for SN-ICP-MS measurements at Utrecht University. Bernhard Schnetger is thanked for the analysis of the glass bead XRF samples at ICBM in Oldenburg. Jack Middelburg and Anne Roepert are thanked for discussions on the statistical processing of the data. This research is made possible by financial support of the PALM-project (820.01.005) by NWO.

References

Aitchison, J., Egozcue, J.J., 2005. Compositional data analysis: where are we and where should we be heading? Math. Geol. 37 (7), 829–850.
Berglund, M., Wieser, M.E., 2011. Isotopic compositions of the elements 2009 (IUPAC technical report). Pure Appl. Chem. 83 (2), 397–410.
Cromwell, E.F., Arrowsmith, P., 1995. Fractionation effects in laser ablation inductively coupled plasma mass spectrometry. Appl. Spectrosc. 49 (11), 1652–1660.
Durrant, S.F., 1992. Multi-elemental analysis of environmental matrices by laser ablation inductively coupled plasma mass spectrometry. Analyst 117 (10), 1585–1592.
Durrant, S.F., Ward, N.I., 2005. Recent biological and environmental applications of laser ablation inductively coupled plasma mass spectrometry (LA-ICP-MS). J. Anal. At. Spectrom. 20 (9), 821–829.
Eggins, S., Kinsley, L., Shelley, J., 1998. Deposition and element fractionation processes during atmospheric pressure laser sampling for analysis by ICP-MS. Appl. Surf. Sci. 127, 278–286.

Fryer, B.J., Jackson, S.E., Longerich, H.P., 1995. The design, operation and role of the laser-ablation microprobe coupled with an inductively coupled plasma-mass spectrometer (LAM-ICP-MS) in the earth sciences. Can. Mineral. 33, 303–306.
Gray, A.L., Williams, J.G., 1987. Oxide and doubly charged ion response of a commercial inductively coupled plasma mass spectrometry instrument. J. Anal. At. Spectrom. 2 (1), 81–82.
Guillong, M., Günther, D., 2002. Effect of particle size distribution on ICP-induced elemental fractionation in laser ablation-inductively coupled plasma-mass spectrometry. J. Anal. At. Spectrom. 17 (8), 831–837.
Günther, D., Frischknecht, R., Heinrich, C.A., Kahlert, H.-J., 1997. Capabilities of an argon fluoride 193 nm excimer laser for laser ablation inductively coupled plasma mass spectrometry microanalysis of geological materials. J. Anal. At. Spectrom. 12 (9), 939–944.
Günther, D., Audétat, A., Frischknecht, R., Heinrich, C.A., 1998. Quantitative analysis of major, minor and trace elements in fluid inclusions using laser ablation-inductively coupled plasma mass spectrometry. J. Anal. At. Spectrom. 13 (4), 263–270.
Gurevich, E.L., Hergenroder, R., 2007. A simple laser ICP-MS ablation cell with wash-out time less than 100 ms. J. Anal. At. Spectrom. 22 (9), 1043–1050.
Jarvis, K.E., Williams, J.G., 1993. Laser ablation inductively coupled plasma mass spectrometry (LA-ICP-MS): a rapid technique for the direct, quantitative determination of major, trace and rare-earth elements in geological samples. Chem. Geol. 106 (3–4), 251–262.
Jenner, G.A., Longerich, H.P., Jackson, S.E., Fryer, B.J., 1990. ICP-MS — a powerful tool for high-precision trace-element analysis in Earth sciences: evidence from analysis of selected U.S.G.S. reference samples. Chem. Geol. 83 (1–2), 133–148.
Jilbert, T., Slomp, C.P., 2013. Rapid high-amplitude variability in Baltic Sea hypoxia during the Holocene. Geology 41 (11), 1183–1186.
Jilbert, T., de Lange, G., Reichart, G.J., 2008. Fluid displacive resin embedding of laminated sediments: preserving trace metals for high-resolution paleoclimate investigations. Limnol. Oceanogr. Methods 6, 16–22.
Jilbert, T., Reichart, G.J., Mason, P., de Lange, G.J., 2010. Short-time-scale variability in ventilation and export productivity during the formation of Mediterranean sapropel S1. Paleoceanography PA4232.
Jochum, K.P., Weis, U., Stoll, B., Kuzmin, D., Yang, Q., Raczek, I., Jacob, D.E., Stracke, A., Birbaum, K., Frick, D.A., Günther, D., Enzweiler, J., 2011. Determination of reference values for NIST SRM 610–617 glasses following ISO guidelines. Geostand. Geoanal. Res. 35 (4), 397–429.
Košler, J., Wiedenbeck, M., Wirth, R., Hovorka, J., Sylvester, P., Miková, J., 2005. Chemical and phase composition of particles produced by laser ablation of silicate glass and zircon—implications for elemental fractionation during ICP-MS analysis. J. Anal. At. Spectrom. 20 (5), 402–409.
Kroslakova, I., Günther, D., 2007. Elemental fractionation in laser ablation-inductively coupled plasma-mass spectrometry: evidence for mass load induced matrix effects in the ICP during ablation of a silicate glass. J. Anal. At. Spectrom. 22 (1), 51–62.
Kuhn, H.-R., Gunther, D., 2004. Laser ablation-ICP-MS: particle size dependent elemental composition studies on filter-collected and online measured aerosols from glass. J. Anal. At. Spectrom. 19 (9), 1158–1164.
Lenz, C., Behrends, T., Jilbert, T., Silveira, M., Slomp, C.P., 2014. Redox-dependent changes in manganese speciation in Baltic Sea sediments from the Holocene thermal maximum: an EXAFS, XANES and LA-ICP-MS study. Chem. Geol. 370, 49–57.
Liu, Y., Hu, Z., Gao, S., Günther, D., Xu, J., Gao, C., Chen, H., 2008. In situ analysis of major and trace elements of anhydrous minerals by LA-ICP-MS without applying an internal standard. Chem. Geol. 257 (1–2), 34–43.
Longerich, H.P., Jackson, S.E., Gunther, D., 1996. Laser ablation inductively coupled plasma mass spectrometric transient signal data acquisition and analyte concentration calculation. J. Anal. At. Spectrom. 11 (9), 899–904.
Lotter, A.F., Lemcke, G., 1999. Methods for preparing and counting biochemical varves. Boreas 28 (2), 243–252.
Mank, A.J.G., Mason, P.R.D., 1999. A critical assessment of laser ablation ICP-MS as an analytical tool for depth analysis in silica-based glass samples. J. Anal. At. Spectrom. 14 (8), 1143–1153.
Mason, P.R.D., Mank, A.J.G., 2001. Depth-resolved analysis in multi-layered glass and metal materials using laser ablation inductively coupled plasma mass spectrometry (LA-ICP-MS). J. Anal. At. Spectrom. 16 (12), 1381–1388.
Perkins, W.T., Fuge, R., Pearce, N.J.G., 1991. Quantitative analysis of trace elements in carbonates using laser ablation inductively coupled plasma mass spectrometry. J. Anal. At. Spectrom. 6 (6), 445–449.
Perkins, W.T., Pearce, N.J.G., Jeffries, T.E., 1993. Laser ablation inductively coupled plasma mass spectrometry: a new technique for the determination of trace and ultra-trace elements in silicates. Geochim. Cosmochim. Acta 57 (2), 475–482.
Pike, J., Kemp, A.E.S., 1996. Preparation and analysis techniques for studies of laminated sediments. Geol. Soc. Lond., Spec. Publ. 116 (1), 37–48.
Pisonero, J., Fernandez, B., Gunther, D., 2009. Critical revision of GD-MS, LA-ICP-MS and SIMS as inorganic mass spectrometric techniques for direct solid analysis. J. Anal. At. Spectrom. 24 (9), 1145–1160.
Reitz, A., Thomson, J., De Lange, G.J., Hensen, C., 2006. Source and development of large manganese enrichments above eastern Mediterranean sapropel S1. Paleoceanography 21, PA3007.
Schnetger, B., Brumsack, H.J., Schale, H., Hinrichs, J., Dittert, L., 2000. Geochemical characteristics of deep-sea sediments from the Arabian Sea: a high-resolution study. Deep-Sea Res. II Top. Stud. Oceanogr. 47 (14), 2735–2768.
Shaheen, M.E., Fryer, B.J., 2011. A simple solution to expanding available reference materials for laser ablation inductively coupled plasma mass spectrometry analysis: applications to sedimentary materials. Spectrochim. Acta B At. Spectrosc. 66 (8), 627–636.
Van Dijk, D., Houba, V.G.J., 2000. Homogeneity and stability of materials distributed by the Wageningen Evaluation Programmes for analytical laboratories. Commun. Soil Sci. Plant Anal. 31, 1745–1756.
Wang, Z., Hattendorf, B., Günther, D., 2006. Analyte response in laser ablation inductively coupled plasma mass spectrometry. J. Am. Soc. Mass Spectrom. 17 (5), 641–651.
Warning, B., Brumsack, H.J., 2000. Trace metal signatures of eastern Mediterranean sapropels. Palaeogeogr. Palaeoclimatol. Palaeoecol. 158 (3–4), 293–309.
Weltje, G.J., Tjallingii, R., 2008. Calibration of XRF core scanners for quantitative geochemical logging of sediment cores: theory and application. Earth Planet. Sci. Lett. 274 (3–4), 423–438.